Eur. Phys. J. B **25**, 217–222 (2002)
DOI: 10.1140/epjb/e20020024

THE EUROPEAN PHYSICAL JOURNAL B
EDP Sciences

Modeling and simulations of the behavior of glass particles in a rotating drum in heptane and water vapor atmospheres

N. Olivi-Tran[1,a], N. Fraysse[2], P. Girard[3], M. Ramonda[4], and D. Chatain[5]

[1] INLN, UMR 6618, Université de Nice-Sophia-Antipolis, 1361 route des lucioles, 06560 Valbonne, France
[2] LPMC, UMR 6622, Université de Nice-Sophia-Antipolis, Parc Valrose, 06108 Nice Cedex 2, France
[3] LAIN, UMR 5011, Université Montpellier II, Place E. Bataillon, 34095 Montpellier Cedex, France
[4] LMCP, Université Montpellier II, Place E. Bataillon, 34095 Montpellier Cedex, France
[5] CRMC2-CNRS[b], campus de Luminy, 13288 Marseille Cedex, France

Received 25 May 2001 and Received in final form 31 October 2001

Abstract. This paper presents a molecular dynamics simulation of an experiment on the stability of a pile of glass beads in a rotating drum filled with a "humid" atmosphere. The experimental avalanche angles were found to be different whether the humidity came from water or heptane. These experimental results allow us to set the basic hypothesis of the modeling: in the heptane atmosphere the glass beads are connected by deformable liquid bridges, whereas in the case of a water atmosphere solid bridges form between the beads. The numerical calculations of the avalanche angle as a function of the undersaturated pressure of heptane or water are in good agreement with the experimental results.

PACS. 45.70.-n Granular systems – 61.43.Bn Structural modeling: serial-addition models, computer simulation

1 Introduction

Dry granular materials have been a broad subject of interest for physicists since the 80' [1]. However, in natural conditions, such as those in geophysics or in material science, the grains are usually not dry because of the humidity of the air. In a wet atmosphere, or more generally in the presence of an interstitial liquid, granular materials become cohesive. Several recent studies performed on spherical beads [2–6] have quantified this qualitatively well-known behavior. However, simple capillary liquid bridges connecting ideal beads do not explain the experimental features.

In a previous paper [4], one of the authors reported quantitative measurements of the maximal stability angle of a pile made of wet glass beads. The "avalanche" angle was measured using the rotating drum method; the experiments were performed under accurately-controlled humidity conditions set by the relative vapor pressure of an under-saturated vapor. The present paper will focus on the following experimental result [4]: the increase of the avalanche angle with the degree of humidity was found to behave differently whether the granular medium had been humidified by a vapor of water or heptane. Simple arguments based on the difference in surface tension for these two liquids cannot account for the qualitative difference between the experimental curves. Note that no dependence of the avalanche angle on the waiting time (resting time of the pile at constant vapor pressure) was observed; differences in the experimental procedures may explain this discrepancy with [3].

In this paper, we present molecular dynamics simulations of a 2D rotating drum with two different models: one for heptane and one for water. In a heptane atmosphere, liquid bridges are supposed to form between the microasperities of the beads leading to an increasing cohesion as the heptane pressure increases [7]. In a water atmosphere, the cohesion of the pile is supposed to result from the formation of solid bridges between the particles due to chemical reactions between water and glass [8].

The numerical models for liquid bridges and solid bridges are presented in Section 2. Numerical results are displayed in Section 3 and compared with the experiments *via* a calculation linking simulations parameters and experimental parameters. Section 4 details the chemical reaction between glass and water. Concluding remarks are presented in Section 5. Two appendices are added to this paper. Appendix A shows AFM images of the surface topography of glass beads. Appendix B displays a solid

[a] e-mail: olivi@inln.cnrs.fr
[b] Laboratoire propre du CNRS, associé aux Universités d'Aix-Marseille 2 et 3

bridge formed between two glass beads by the reaction between water and glass in air (Scanning Electron Microscopy).

2 Numerical simulations

2.1 Numerical model without cohesion

Molecular dynamics is a powerful numerical method to study the dynamics of granular materials [10]. The model we used here is a modified version of molecular dynamics for granular flow without cohesion in a two-dimensional rotating cylindrical drum [10–12]. With this method, a two-dimensional cross-section of the experimental system is studied. The pile of glass beads is modeled as N disks of equal density and diameter located in a two-dimensional rotating drum of diameter D. The particle-particle and particle-wall contacts are described by a Hooke-like force law in the normal direction (*i.e.* in the particles' center-center direction). Then the force is written:

$$\mathbf{F}_n(i,j) = \left(-\left[Y r_{\text{eff}} \frac{1}{2}(d_i + d_j) - |\mathbf{r}_{i,j}| \right] + \gamma \frac{m_{\text{eff}}(\mathbf{v}_{i,j} \cdot \mathbf{r}_{i,j})}{r_{\text{eff}} |\mathbf{r}_{i,j}|} \right) \frac{\mathbf{r}_{i,j}}{|\mathbf{r}_{i,j}|}, \quad (1)$$

where Y is the Young modulus, $r_{\text{eff}}(m_{\text{eff}})$ stands for the effective radius (mass) of the 2 disks, d_i (resp. d_j) is the diameter of particle i (resp. j) and $r_{i,j}$ points from particle i to particle j. γ is a phenomenological dissipation coefficient and $v_{i,j} = v_i - v_j$, the relative velocity of particle j toward particle i.

When cylindrical disks are used in the simulation as an approximation to describe non cylindrical particles, a real static friction has to be included. We model this by putting a virtual spring at the point of first contact [10,11]. Its elongation is integrated over the entire collision time and set to zero when the contact is lost. The maximum possible value of the restoring force in the shear direction (*i.e.* perpendicular to the normal direction), according to Coulomb's criterion, is proportional to the normal force multiplied by the friction coefficient μ. Cast into equation (1), this gives a friction force $\mathbf{f}_s(i,j)$ which is written:

$$\mathbf{f}_f(i,j) = -k_s \int (\dot{r}_i - \dot{r}_j)\mathbf{s}\mathrm{d}t, \quad (2)$$

$$\mathbf{f}_s(i,j) = -\text{sign}(f_j(i,j)) \min(f_f(i,j), \mu |f_n(i,j)|)\mathbf{s}, \quad (3)$$

where $\mathbf{s}$ stands for the unit vector in the shear direction. The rotational force $\mathbf{f}_r(i,j)$ exerted by particle j on particle i is calculated by:

$$\mathbf{f}_r(i,j) = \mathbf{f}_s(i,j) \cdot d_i/2. \quad (4)$$

When a particle collides with the cylinder wall the same forces act, as in equations (1) and (3), as if this particle had encountered another particle with infinite mass and radius. The only external force acting on the system results from gravity, $g = 9.81$ ms^{-2}.

2.2 Numerical model with capillary interaction

It is well known that the capillary force between two smooth beads in contact and connected by a liquid bridge decreases with the volume of the bridge [9]. As the experimental results on the stability of a pile of wet spherical grains do not obey this rule, many authors suggested that the surface of the beads was rough [2,3,7] and that the liquid bridge between two beads was actually formed between a cone and a plate, *i.e.* between an asperity of one of the beads and a smooth part of the other. In this case, the capillary force increases with the volume of the liquid bridge (for contact angles $< \pi/2$). In Appendix A, the AFM images of a glass bead indeed displays outward conical defects.

In order to compute the behavior of the avalanche angle in the rotating drum as a function of the undersaturated vapor pressure of heptane, the molecular dynamics code for dry particles has been slightly modified. The calculation of the shear force remains identical but a spring force needs to be added to the normal forces; it is given by the following equation:

$$f_{\text{cap}} = K r_{\text{eff}} \frac{1}{2}(d_i + d_j) \quad (5)$$

where K is the additive spring constant. K depends on the surface tension and on the viscosity of the liquid. But more importantly, simulations are performed using increasing values of K in order to account for the increasing cohesion due to the increasing relative humidity. This last point will be detailed in 3.2.

This force is different from the Hooke-like force for dry beads, because it still has a finite value when the disks are no longer in contact. This added force is set to zero when the distance between the centers of the disks is equal to the diameter of one disk and increases as a linear spring force until the spring has a length equal to a maximum length of 10% of the disk's radius.

2.3 Numerical model with solid interactions

It is assumed that chemical reactions between water and glass produce solid bridges between the particles in the rotating drum. Figure 4 shows a picture of a solid bridge obtained as described in Appendix B (Scanning Electron Microscopy). In order to take into account the presence of solid bridges between disks in the numerical simulations, constant forces are added to the normal force and to the shear force at each time step. These additional normal and shear forces are considered equal and denoted F. They have a threshold directly proportional to the section of the solid bridge, as the solid bridge breaks along its cross-section. As for K, simulations are performed using increasing values of F. For more details, see Section 3.2.

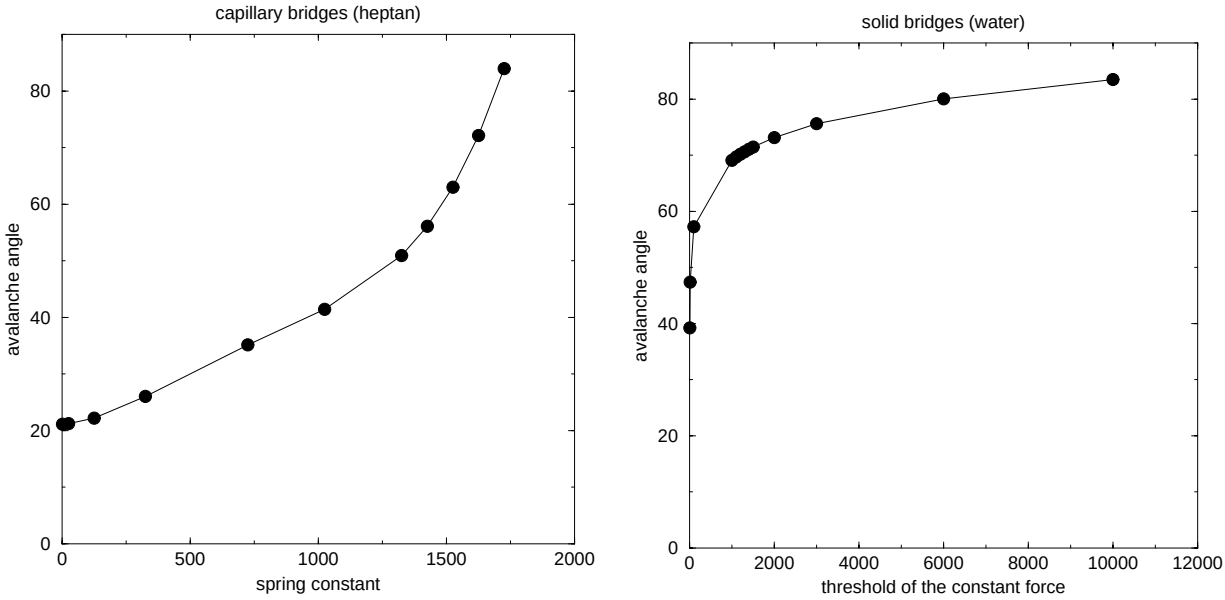

Fig. 1. (a) Numerical results of the avalanche angle (in degrees) as a function of the additive spring constant, K, for capillary bridges between the disks (heptane case). (b) Numerical results of the avalanche angle (in degrees) as a function of the additive constant force, F, for solid bridges between the disks (water case).

3 Results

3.1 Results depending on the added forces

870 disks of diameter 1 were put in a rotating drum of diameter 120. The results were averaged over 40 simulations for each value of the spring constant K or of the force F. Figures 1a and 1b present the molecular dynamics simulations of the avalanche angle for particles connected by liquid bridges and solid bridges, respectively. Figure 1a is a plot of the avalanche angle as a function of the additive spring constant, K, induced by the liquid bridges while Figure 1b is a plot of the avalanche angle as a function of the constant force F induced by the solid bridges. Each value of K (resp. F) corresponds to one value of the relative humidity.

The two curves have different shapes: for the liquid bridge case, the avalanche angle as a function of the added spring constant increases with a positive curvature, and for the solid bridge case, the avalanche angle increases first rapidly and then saturates at 90°. It is not possible to compare the two curves directly as the avalanche angle is not expressed as a function of the same parameter. In the next section, we will plot the avalanche angle as a function of the same parameter, *i.e.* the relative humidity ratio.

3.2 Comparison of numerical results with experimental results

In order to be able to compare numerical simulations with the experimental data in [4], the spring constant (for heptane) and the constant force threshold (for water) have to be written as a function of the relative undersaturated vapor pressure.

If we call ℓ the radius of the capillary bridge, R the radius of the microasperities, and r_c the radius of curvature of the meniscus, and with the hypothesis that $R \gg \ell \gg r_c$, the volume V of the liquid bridge can be written, knowing that $\ell^2 \propto Rr_c$:

$$V \propto \ell^2 r_c \propto R r_c^2. \tag{6}$$

Following Kelvin's law, this volume can be written, with the under-saturated vapor pressure P_v and the saturated vapor pressure P_{sat}:

$$V \propto 1/\mathrm{Log}^2(P_v/P_{sat}) \cdot \tag{7}$$

The relation between the volume of the liquid bridge and the relative humidity rate is therefore:

$$V \propto 1/\mathrm{Log}^2(RH) \tag{8}$$

where RH is the relative humidity rate. Now, supposing that the spring constant K in our numerical simulation with liquid bridges is proportional to the volume V of the liquid bridges, RH can be written, as a function of K:

$$RH = \exp(-C/K^{1/2}) \tag{9}$$

where C is a free parameter in our simulations.

In Figure 2a, both the experimental and numerical results for a heptane atmosphere are plotted for $C = 5$. They are in good agreement.

In the case of solid bridges, the constant force F depends on the cross-section of the solid bridges. The solid bridges' cross-section is supposed to be proportional to the

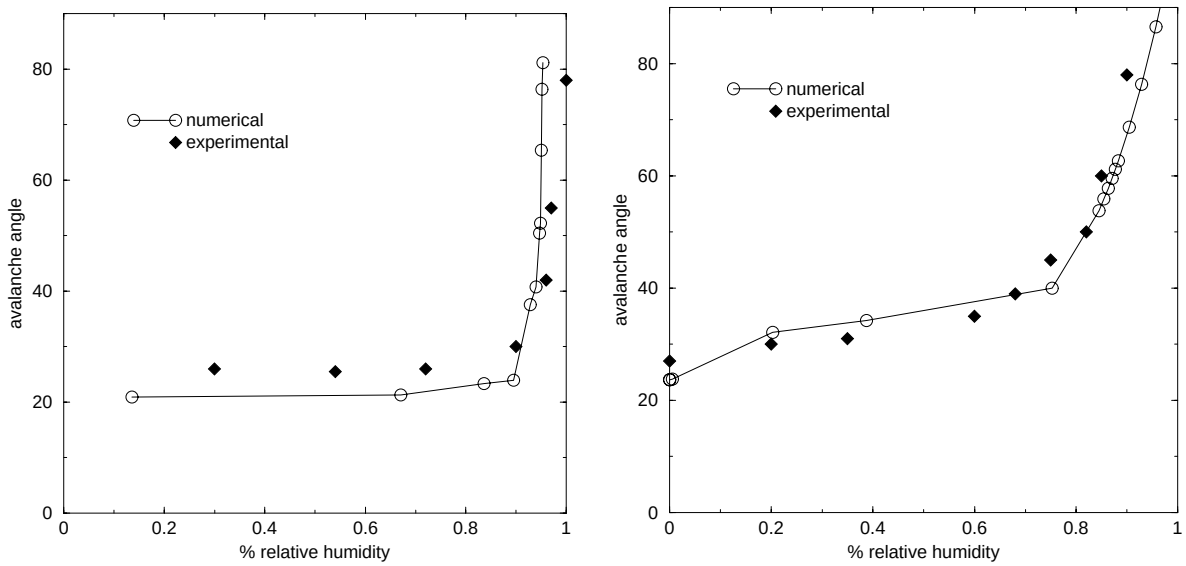

Fig. 2. (a) Numerical results and experimental results of the avalanche angle (in degrees) as a function of the relative humidity ratio, RH, for capillary interactions between the particles (heptane case). (b) Numerical results and experimental results of the avalanche angle (in degrees) as a function of the relative humidity ratio, RH, for solid bridges between the particles (water case).

cross-section of the liquid bridges which existed before solidification occured. So we have the section $S \propto \ell^2 \propto Rr_c$ and:

$$S \propto 1/\mathrm{Log}(P_v/P_{sat}) \cdot \tag{10}$$

Thus:

$$RH = \exp(-D/F) \cdot \tag{11}$$

In Figure 2b, experimental and numerical results are plotted for water vapor for $D = 40$. Again, a good agreement is obtained.

4 Discussion

It is well established that the formation of capillary bridges between the glass beads (for instance when surrounded by an under-saturated heptane vapor), produces an attractive force which increases when the volume of the bridges increases [7]. This is because the bridges form between two peaks on the surface of two beads in contact or at least between one peak on one surface and a flat part on the other surface. On the other hand, it is unusual in the literature of granular materials to consider that water reacts with glass. A precise description of the chemical reactions involved has been performed in reference [8]. A summary of these reactions is given below. The composition of the glass of the beads used in the experiments is given in Table 1. The alkaline cations of the glass, such as sodium, react with the H_3O^+ ions of water by a rapid inter-diffusion process. The chemical reaction is the following:

$$\equiv \mathrm{Si} - \mathrm{O}^-\mathrm{Na}^+ + \mathrm{H_3O}^+ \rightarrow \equiv \mathrm{Si} - \mathrm{O} - \mathrm{H} + \mathrm{H_2O} + \mathrm{Na}^+. \tag{12}$$

Table 1. Composition of the sodo-silicate glass.

SiO_2	Na_2O	CaO	MgO	Al_2O_3	Fe_2O	K_2O
72.5%	13.7%	9.8%	3.3%	0.4%	0.2%	0.1%

The surface of glass becomes poorer in sodium and richer in water and silanol ions. This mechanism obeys a Fick diffusion law and is valid for any other alkaline ions. This diffusion phenomenon is supposed to be very rapid, mostly because of the sodium ions, which react strongly with water. The surface of the glass becomes more and more hydrated and porous, and forms what is generally called a microporous silica gel. This silica gel is able to connect two particles by creating $\mathrm{Si} - \mathrm{O} - \mathrm{Si}$ bonds between the two particles: the gel contains enough $\mathrm{Si}-\mathrm{OH}$ bonds (hydrated silica) to form a bridge between two beads in contact according to the following polycondensation process:

$$\equiv \mathrm{Si} - \mathrm{OH} + \mathrm{HO} - \mathrm{Si} \equiv \rightarrow \equiv \mathrm{Si} - \mathrm{O} - \mathrm{Si} \equiv + \mathrm{H_2O}. \tag{13}$$

Further chemical reactions, such as the creation of chemical bonds between the silica gel bridge and other ions, may occur depending on the pH of the water and on the other species present in the liquid water phase. These latter reactions are not essential here since the solid bridge, which has formed inside the capillary bridge, already has its own mechanical action on the granulate: to add ions to the gelled bridge should not significantly improve its resistance to stress. Moreover, the kinetics of these latter reactions are very slow at room temperature, compared to the kinetics of alkaline ion diffusion. Recall that no time dependence was observed experimentally, in agreement with this last point.

In Appendix B, a solid bridge between two particles is displayed on a scanning electron microscopy image

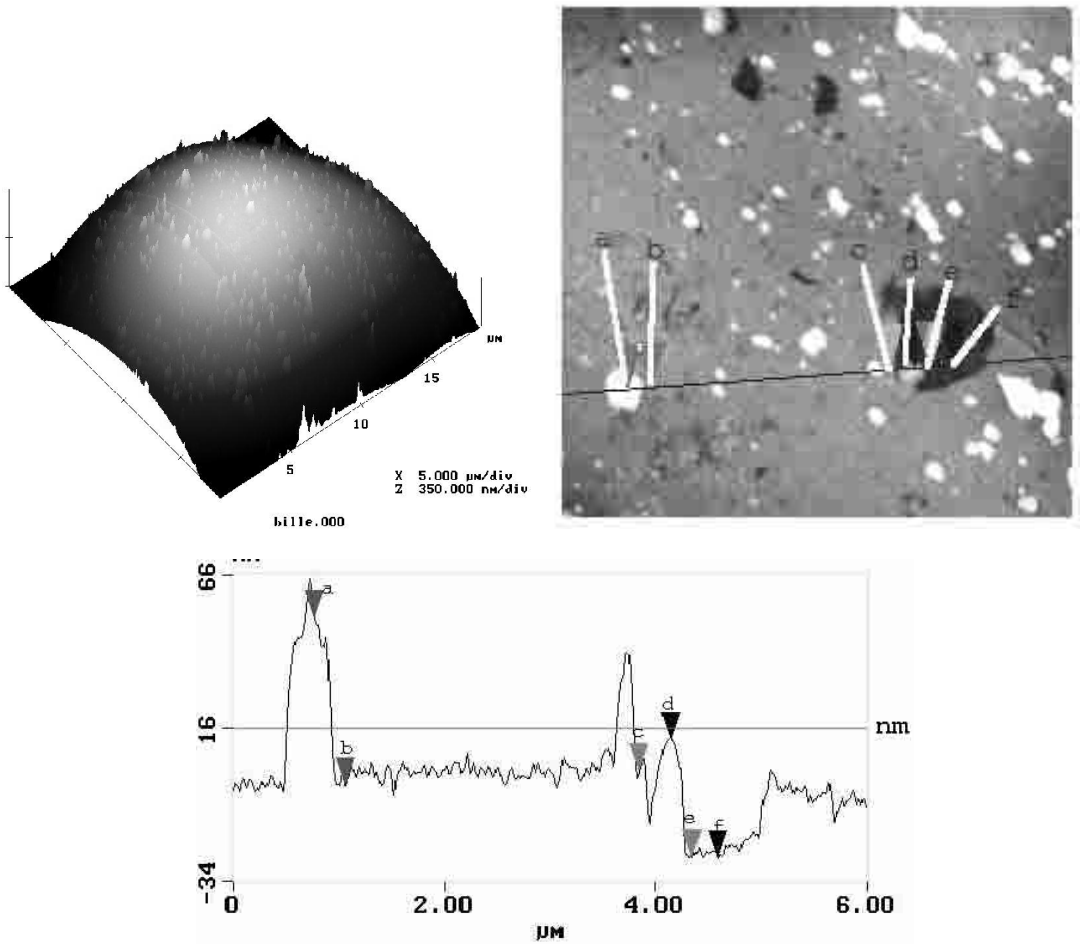

Fig. 3. (a) AFM image of a glass bead. The scales are 5 μm per division in the x- and y-directions and 350 nm per division in the z-direction. (b) Image of the bead surface from the top, the lines and markers correspond to the height profile shown in (c). (c) Height profile showing topographical accidents.

(Fig. 4). This bridge results from an experiment in which the glass beads had been soaked in water, and then dried at 100 °C in air. After drying, the beads remained more or less glued together: it is an indication of the presence of solid bridges. The same experiment performed with heptane yielded no cohesion at all for the beads after drying. This and the fact that experimental and numerical results fit well with the use of only one free parameter (which makes the link between normalized computational values and real experimental data) strengthen our hypothesis of the presence of interparticular solid bridges in the case of water, and of the presence of capillary bridges in the case of heptane vapor.

5 Conclusion

We made the hypothesis here that in a rotating drum experiment with under-saturated heptane vapor, liquid bridges form between the asperities (observed on AFM topographies) of the glass beads. These liquid bridges increase the cohesion of the granulate and hence the avalanche angle as a function of the relative humidity ratio. The numerical and experimental results are in good agreement so this postulate can be accepted as reasonable. Using water vapor instead of heptane, in the same experiment, a different hypothesis was required: micro-solid bridges are formed between the asperities of the glass beads, due to the chemical interaction between glass and water. Once again, simulations and experiments agree very well. Therefore, although the details of the chemistry of (glass + water) is not yet well understood, we think that these solid bridges do exist, as seen on a MEB photograph of two glass beads, as the result of an additional experiment with water and glass beads.

The authors are thankful to Ch. Henrique for providing the original molecular dynamics program.

Appendix A

An AFM analysis of the surface of our beads was performed, in air at room temperature. The results are presented in Figures 3a, b and c. Figure 3a is a reconstruction of part of the surface; Figure 3b is an image of the top view of the surface; Figure 3c shows the heights of the peaks

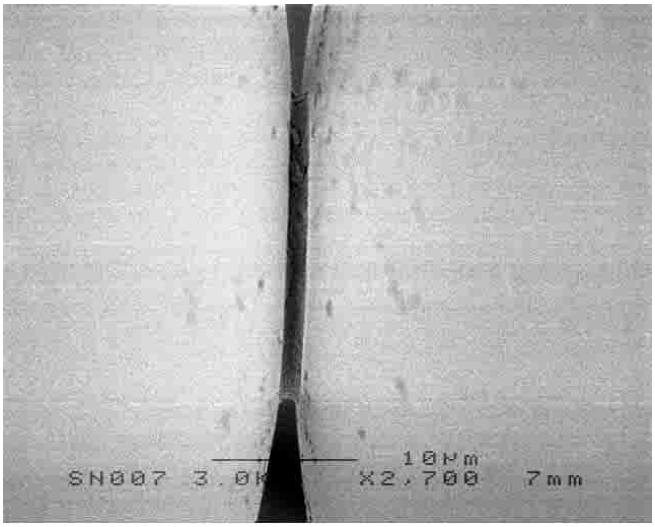

Fig. 4. MEB photograph of a solid bridge between two glass beads (magnification ×2700).

of the surface along a scanning line. The surface of the glass beads we use presents typical microasperities with a height of a few nanometers. These defects are sufficient to produce liquid microbridges leading to an increasing capillary force when the volume of liquid increases.

Appendix B

An experiment was performed as a test of the occurrence of chemical reactions between the sodo-silicate glass beads we use and water. Glass particles were soaked in water for 12 hours and then dried in an oven at 100 °C. Figure 4 displays a solid bridge between two glass beads as observed by scanning electron microscopy.

These experimental conditions are slightly different from the ones used in the rotating drum with water vapor. However, the chemical reactions are similar with the chemical potential of water in the rotating drum smaller than during immersion of the glass particles.

References

1. P.G. de Gennes, Rev. Mod. Phys. **71**, S374 (1999).
2. D.J. Hornbaker, R. Albert, I. Albert, A.-L. Barabási, P. Schiffer, Nature **387**, 765 (1997); R. Albert, I. Albert, D.J. Hornbaker, P. Schiffer, A.-L. Barabási, Phys. Rev. E **56**, R6271 (1997); P. Tegzes, R. Albert, M. Paskvan, A.-L. Barabási, T. Vicsek, P. Schiffer, Phys. Rev. E **60**, 5823 (1999).
3. L. Bocquet, E. Charlaix, S. Ciliberto, J. Crassous, Nature **396**, 735 (1998).
4. N. Fraysse, H. Thomé, L. Petit, Eur. Phys. J. B **11**, 615 (1999); N. Fraysse, L. Petit, Mat. Res. Soc. Symp. Proc. **627**, BB7.1.1 (2000).
5. T.G. Mason, A.J. Levine, D. Ertas, T.C. Halsey, Phys. Rev. E **60**, R5044 (1999).
6. A. Samadani, A. Kudrolli, Phys. Rev. E **64**, 051301 (2001).
7. T.C. Halsey, A.J. Levine Phys. Rev. Lett. **80**, 3141 (1998).
8. L.L. Hench, D.E. Clark, J. Non-Crystalline Solids **28**, 83 (1978); H. Scholze, J. Non-Crystalline Solids **102**, 1 (1988); P. Chartier, Verre **3**, 5 (1997).
9. See for instance: R.B. Heady, J.W. Cahn, Metall. Trans. **1**, 185 (1970).
10. G.H. Ristow, *Granular Dynamics: a Review about recent Molecular Dynamics Simulations of Granular Materials*, in *Annual Reviews of Computational Physics*, edited by D. Stauffer (World Scientific, 1994), Vol. I, p. 275.
11. G.H. Ristow, Europhys. Lett. **34**, 263 (1996).
12. T. Elperin, A. Vikhansky, Europhys. Lett. **42**, 619 (1998).